QCD AND TOP-QUARK RESULTS FROM THE TEVATRON*

Marek Zieliński

University of Rochester, Department of Physics & Astronomy
Bausch & Lomb Hall, P.O. Box 270171
600 Wilson Boulevard Rochester, NY 14627-0171, USA

(Received November 15, 2006)

Selected recent QCD and top-quark results from the Tevatron are reviewed, aiming to illustrate progression from basic studies of QCD processes to verification of perturbative calculations and Monte Carlo simulation tools, and to their applications in more novel and complex cases, like top-quark studies and searches for new physics.

PACS numbers: 12.38.Qk, 13.85.Rm, 13.87.–a, 14.65.Ha

1. QCD results

QCD processes provide signals to test theoretical calculations and models and contribute major backgrounds to many measurements. Thus, their detailed understanding and modeling is of crucial importance.

Production of isolated photons at large p_{T} provides one of the cleanest and most accurate tests of perturbative QCD (pQCD). Such photons originate primarily from hard collisions of partons (quark–gluon or quark–antiquark) and are thus sensitive to the parton distribution functions (PDFs). Consequently, they can help constrain PDFs (especially the large-x gluon distribution) independently of the high-p_{T} jet production. Such constraints can reduce ambiguities in interpreting results on high-p_{T} jet production in terms of new physics. Isolated photon samples also provide indispensable calibration of the recoiling jets. D0 presented the first measurement of the inclusive isolated photon cross section in Run 2 of the Tevatron [1]. The photon spectrum, obtained using 326 pb^{-1}, spans p_{T}= 23–300 GeV/c and $|\eta| < 0.9$, significantly extending the reach observed in Run 1. The measurement agrees well with next-to-leading order (NLO) pQCD calculation [2] over six orders of magnitude, Fig. 1 (left). The data/theory ratio, presented

* Presented at the "Physics at LHC" Conference, Kraków, Poland, July 3–8, 2006.

in the right panel, shows that the theoretical scale dependence and PDF uncertainties are comparable to the experimental error bars. Further improvements in theoretical predictions are desired to reduce the level of sensitivity to the choice of pQCD scales in order to fully exploit the potential of this measurement for constraining PDFs with the help of much larger data samples already available.

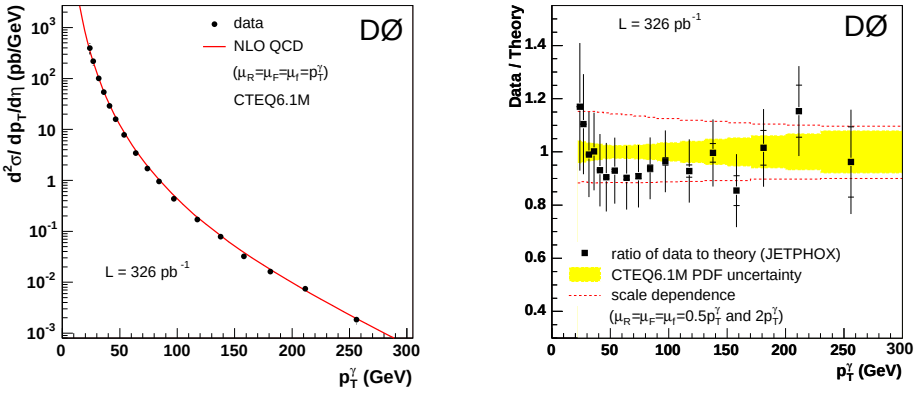


Fig. 1. Left: Inclusive isolated-γ cross section *versus* p_{T}. Right: Ratio to NLO pQCD.

Measurements of the inclusive jet cross section provide tests of pQCD and sensitivity to new physics by probing distances down to $\approx 10^{-19}$ m. Results at large rapidities are particularly important for constraining PDFs in a kinematic region where no effects from new physics are expected. CDF obtained the first measurement in Run 2 of inclusive jet cross section in five rapidity regions using the longitudinally-invariant k_{T} algorithm and ≈ 1 fb^{-1} of data [3]. Fig. 2 (top) shows the results for the size parameter $D = 0.7$ for jets with $p_{\mathrm{T}} > 54$ GeV/c and $|y| < 2.1$. The bottom panel shows the data ratio to NLO theory [4] and displays the experimental and theoretical uncertainties. The former are dominated by the jet energy calibration and the latter by the QCD scale and PDF variations. The theoretical calculations include corrections for non-perturbative effects related to the underlying event and hadronization process. These corrections are essential to obtain good agreement between data and theory. Similar level of agreement has been found for central jets ($0.1 < |y| < 0.7$) using values of $D = 0.5$ and 1.0 and the corresponding corrections. These results demonstrate veracity of the k_{T} algorithm in the hadron-collider environment within the range of the measurement. For the most forward rapidity bin ($1.6 < |y| < 2.1$) the

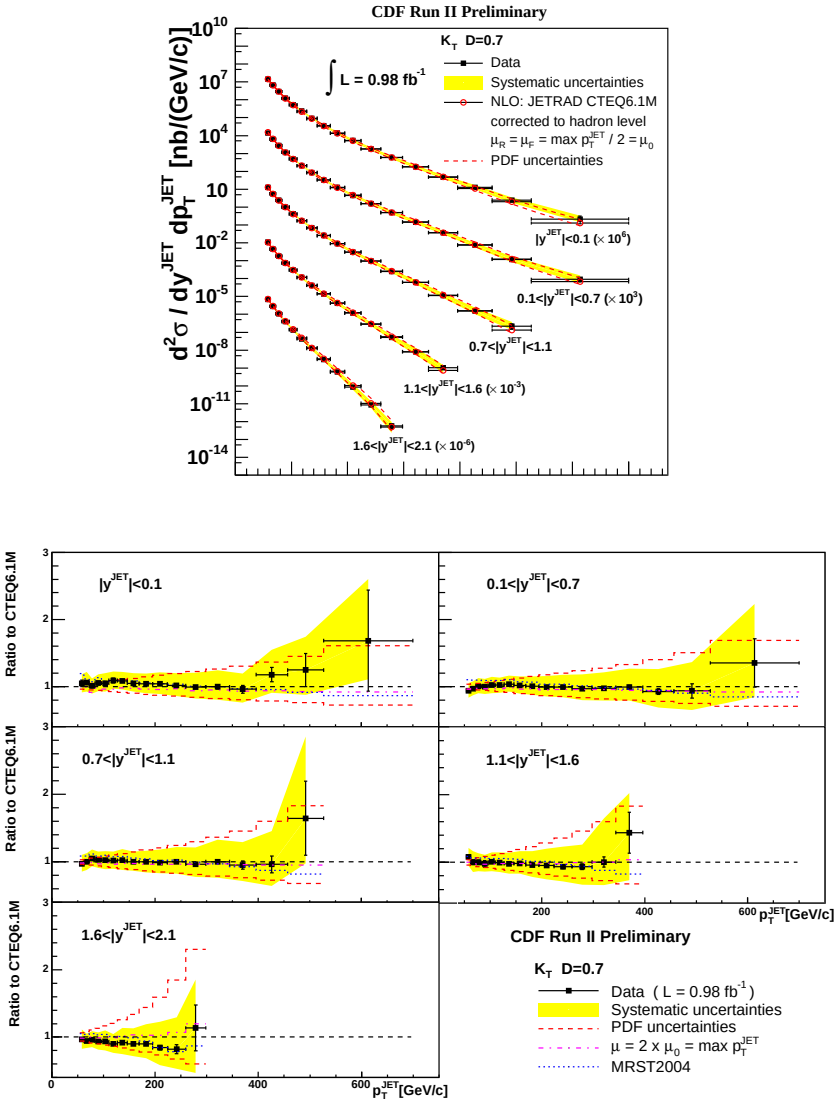


Fig. 2. Top: Inclusive k_{T}-jet cross section *versus* p_{T}. Bottom: Ratio to NLO pQCD.

experimental uncertainty is smaller than the one due to PDFs, hence this measurement is expected to further constrain large-x PDFs in future global fits. Similar conclusions have been reached by CDF and D0 for the inclusive jet cross section measurements using the MidPoint cone algorithm (not shown). Here corrections for soft effects are smaller than for k_{T} algorithm but non-negligible at the current level of precision.

Correlations in the azimuthal angle $\Delta\phi$ between the two leading jets in an event provide a clean and simple probe of radiation effects. In the absence of radiation $\Delta\phi = \pi$. Soft radiation causes small deviations from π while $\Delta\phi$ significantly lower than π indicates the presence of hard radiation, such as additional jets with high p_{T}. The proper description of multi-parton radiation is crucial for a wide range of precision measurements as well as for searches for new physical phenomena at Tevatron and LHC. D0 results [5] for $\Delta\phi$ correlations between central jets ($|\eta| < 0.5$) are presented in Fig. 3 in four ranges of leading-jet p_{T}. Since the data are sensitive to a range of jet multiplicities, they provide a test of recent Monte Carlo approaches that combine exact LO pQCD matrix elements for multi-parton production with parton-shower models and of the associated "matching" prescriptions imposed to avoid double-counting of equivalent parton configurations. Two such generators, ALPGEN [6] (not shown) and SHERPA [7], are in good agreement with data, thus enhancing confidence in their applications to other processes. The data are also well described by NLO pQCD for three-jet production [8], and by HERWIG [9] with default parameters. Distributions from PYTHIA [10] are sensitive to the value of a parameter which controls the maximum allowed virtuality in the initial-state shower. The shaded bands in Fig. 3 (right) show the range of predictions when this parameter is varied by a factor of four. The optimal value of 2.5 has been incorporated in the recent tunes DW and DWT of PYTHIA parameters [11].

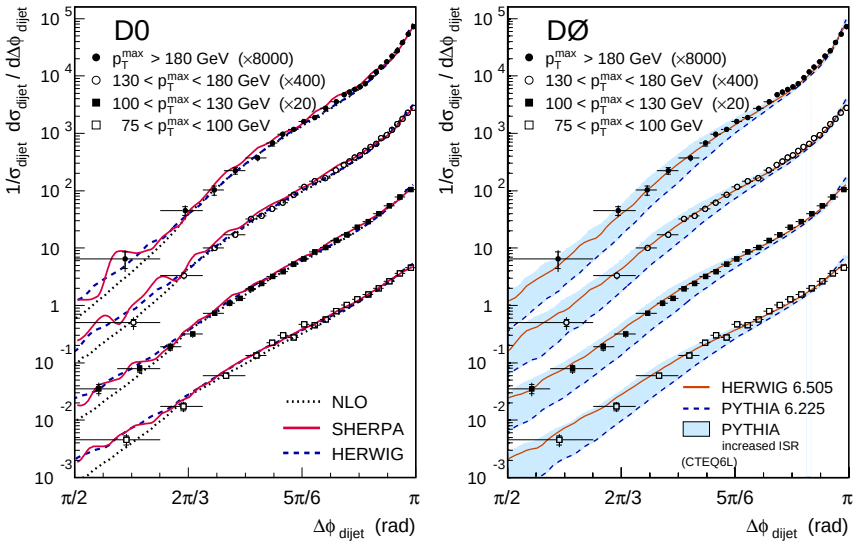


Fig. 3. Left: dijet $\Delta\phi$ distributions compared to NLO pQCD, HERWIG and SHERPA. Right: Comparison to PYTHIA with varied Initial State Radiation (ISR).

Production of W and Z bosons in association with jets constitutes an important background to top-quark production and in the searches for new physics, including production of the Higgs boson and supersymmetric particles. Thus an accurate modeling of this process is essential. The presence of W/Z ensures high Q^2 and facilitates tests of pQCD and Monte Carlo tools for configurations with multiple soft jets. D0 compared predictions from PYTHIA and SHERPA to various distributions in Z/γ^*+jets events using 950 pb^{-1}of data [12]. Data selection required two electrons with $p_{\mathrm{T}}>$ 25 GeV/c and $|\eta| < 2.5$ within a di-electron mass window of 70–100 GeV, and jets with

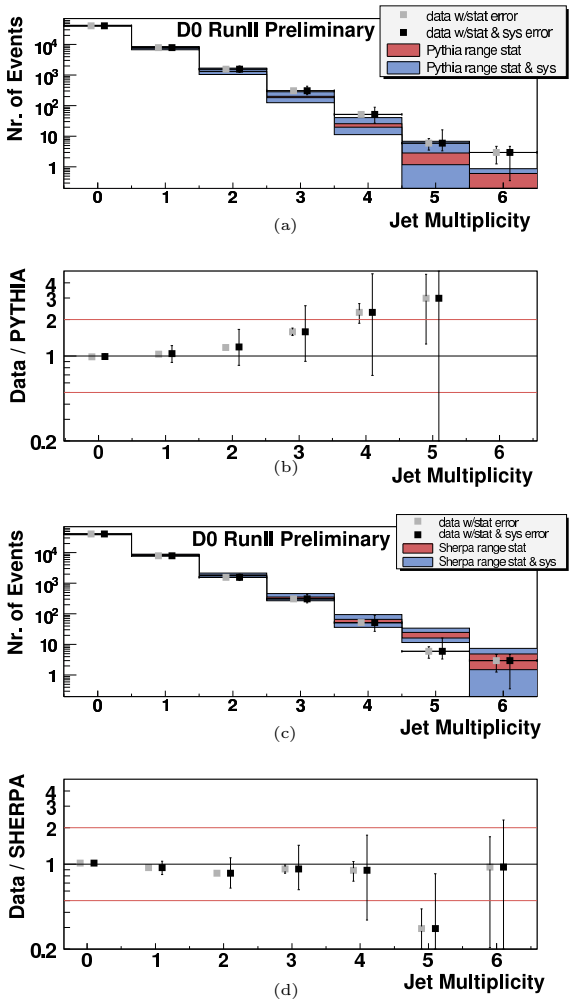


Fig. 4. Jet multiplicity in Z+jets events compared to PYTHIA and SHERPA.

$p_{\mathrm{T}} > 15$ GeV/c. PYTHIA was found to underestimate the production rate of higher jet multiplicities, Fig. 4 (a), (b). SHERPA provides a good description of jet multiplicity (Fig. 4 (c), (d)), and all kinematic distributions studied, including p_{T} distributions of the Z and of 1st, 2nd and 3rd leading jets, as well as $\Delta\phi$ and $\Delta\eta$ angular distributions between the jets. Significant differences with data have been observed for PYTHIA distributions.

Using 320 pb^{-1} of data CDF performed [13] shape comparisons between W+jets production (up to four jets) with predictions from ALPGEN interfaced to PYTHIA for showering and hadronization. Jets were corrected to hadron level and kinematic cuts imposed to reduce model dependence on acceptance and efficiency. Data selection required a good-quality electron candidate with $p_{\mathrm{T}} > 20$ GeV/c, missing transverse energy $\not\!\!E_{\mathrm{T}} > 30$ GeV, and $R = 0.4$ cone jets with $p_{\mathrm{T}} > 15$ GeV/c and $|\eta| < 2$. Reasonable agreement is observed for the jet p_{T} distributions (Fig. 5 (top)), ΔR between jets in W+2jets sample (Fig. 5 (bottom)), and dijet invariant mass (not shown).

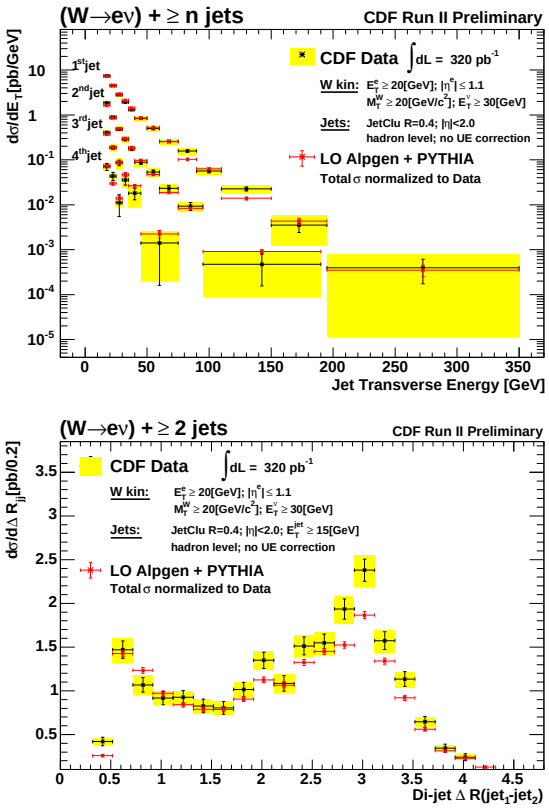


Fig. 5. Jet p_{T} and ΔR in W+jets events compared to ALPGEN.

2. Top-quark results

Ten years after its discovery top quark is intensely studied at the Tevatron. Its surprisingly large mass makes it the only fermion having the Yukawa coupling near unity implying its large contribution to the radiative corrections to the Higgs mass. This leads to speculation that electroweak symmetry breaking mechanism may be probed through studies of its production and properties. Consequently, every aspect of top-quark physics experimentally accessible is vigorously scrutinized at the Tevatron.

The Standard Model (SM) predicts that at the Tevatron top quarks are primarily produced in pairs through the strong force by $q\bar{q}$ annihilation 85% of the time and by gg fusion 15% of the time. The predicted cross section is $\sigma_{t\bar{t}} = 6.77 \pm 0.42$ pb for $m_t = 175$ GeV [14]. In SM, top quarks decay $\approx 100\%$ to Wb, and hence $t\bar{t}$ events are classified according to the decay modes of the W's. In dilepton events both W's decay into e or μ. This channel has a low branching fraction ($\approx 5\%$) but is very clean. A recent extension of the dilepton analysis selects candidate events requiring an isolated track instead of one of the leptons. This improves selection efficiency and enlarges the event sample at the cost of additional backgrounds. The channel when one W decays to e or μ and the other to quarks is called lepton+jets. It has a higher branching fraction ($\approx 30\%$) but also receives higher backgrounds. Since it provides a large but still fairly pure sample of top quarks, it facilitates some of the best measurements in top physics. Decays of both W's to quarks result in the all-hadronic channel, which has the largest branching fraction ($\approx 44\%$) but also the highest background from QCD multi-jet production. The b-tagging information is essential for background suppression in this channel. It also helps to reduce backgrounds in the lepton+jets channel. Analyses based on decay modes involving τ leptons are especially difficult and are only now becoming developed. Due to the presence of W's and jets in top decays, good understanding and simulation of QCD W/Z+jets and multijet production is indispensable in top-quark measurements.

One of the best measurements of $t\bar{t}$ cross section has been obtained by CDF using the lepton+jets channel and 695 pb^{-1} of data [15]. While the traditional analyses in this channel have used selections based on topological variables to enhance $t\bar{t}$ signal, this measurement employs b-tag information to reduce backgrounds. Events are required to have one isolated electron or μ with $p_{\mathrm{T}} > 20$ GeV/c and $\not\!\!E_{\mathrm{T}} > 20$ GeV, at least three jets with $p_{\mathrm{T}} > 15$ GeV/c within $|\eta| < 2$ and the total scalar sum of transverse energies of all objects in the event > 200 GeV (including jets with $p_{\mathrm{T}} > 8$ GeV/c and $|\eta| < 2.4$). The last requirement is dropped for the double-tagged sample. As illustrated in Fig. 6 (left), the events in the "W+3jet" and "$W+\geq$4jet" bins are relatively background free and dominated by $t\bar{t}$ contribution when

one b-tag is required. The resulting cross section is $\sigma_{t\bar{t}} = 8.2 \pm 0.6(\text{stat.}) \pm 1.0(\text{syst.})$ pb. The uncertainty is dominated by systematics, and its largest component comes from b-tagging. When two b-tags are required, the sample statistics is reduced but $t\bar{t}$ purity improves even further. It is noteworthy that the cross section measurement using the double-tagged sample alone has achieved a 5σ significance: $\sigma_{t\bar{t}} = 8.8^{+1.2}_{-1.1}(\text{stat.})^{+2.0}_{-1.3}(\text{syst.})$ pb.

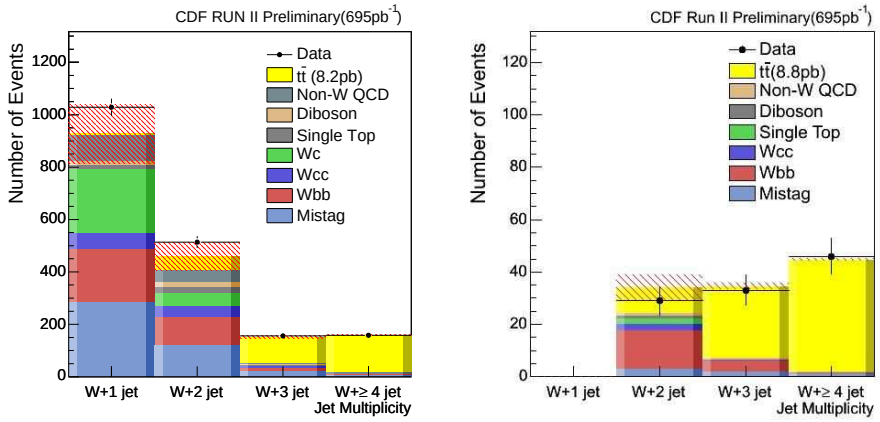


Fig. 6. $t\bar{t}$ and background contributions to W+jets samples with single (left) and double (right) b-tags.

CDF and D0 are developing a variety of techniques to examine $t\bar{t}$ decays into the all-hadronic final state. A novel analysis from D0 [16], based on 360 pb^{-1}, selects six-jet events with at least 2 jets having $p_{\mathrm{T}} > 45$ GeV/c and tagged as b-jets with a secondary-vertex tagging algorithm. The remaining jets are required not to be b-tagged, two of them to have $p_{\mathrm{T}} > 20$ GeV/c and the rest $p_{\mathrm{T}} > 15$ GeV/c. All jets are required to be within $|y| < 2.4$. As no events have been rejected based on the presence of high-p_{T} leptons or $\not\!\!E_{\mathrm{T}}$, this sample includes contributions from the all-hadronic channel, the τ channel with hadronic τ decays, and the other $t\bar{t}$ decay channels when additional jets are produced. The double b-tag requirement is essential for suppressing the QCD backgrounds. The inclusive dijet mass distribution for non b-tagged jets (jj), and the three-jet mass distribution for one b-tagged and two non-tagged jets (bjj) exhibit visible excess of events above a smooth background. This enhancement is interpreted as due to W and top production (Fig. 7). A method has been developed to derive the non-$t\bar{t}$ background directly from the data. After background subtraction the jj and bjj mass distributions agree well with expectations for W and top decays into jets based on PYTHIA and simulation of detector effects. The resulting $t\bar{t}$ cross section of $12.1 \pm 4.9 \pm 4.6$ pb (for $m_t = 175$ GeV) is consistent with SM predictions. Its accuracy is expected to be significantly improved when

larger data samples are analyzed and the technique is further developed. The direct observation of resonant W and top mass peaks in the hadronic mode is reassuring in anticipation of the LHC data.

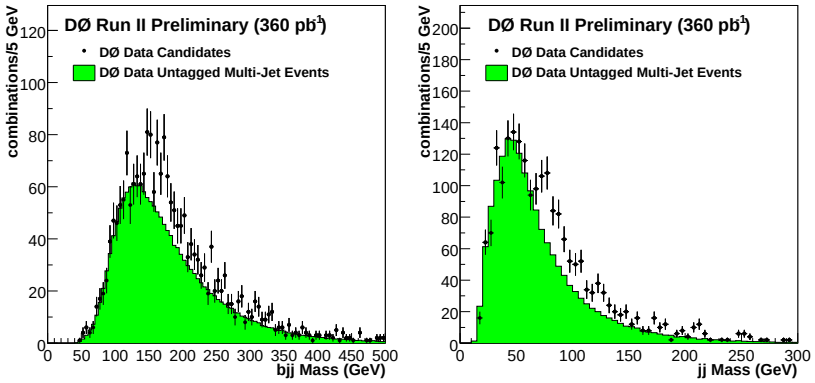


Fig. 7. The dijet mass for non b-tagged jets (jj) (left) and the three-jet mass for one b-tagged and two non b-tagged jets (bjj) (right) with non-$t\bar{t}$ background overlayed.

Fig. 8 shows a summary of recent $t\bar{t}$ cross section measurements by D0 and CDF. The accuracy of the combined result is approaching 10%. With further increase of the data sets, it is becoming possible to test compatibility of the cross sections obtained from different channels.

The top quark mass is a fundamental parameter of the SM and should be measured to the highest possible accuracy. With large data samples now available the measurements are no longer statistically limited. It is therefore important to understand systematic uncertainties in detail and to minimize their impact on the determination of m_t. Since the dominant source of systematic uncertainty has been the jet energy scale (JES), recent analyses employ the *in situ* jet calibration by imposing the well known mass of the W in the reconstruction of the $W \to jj$ decays in the $t\bar{t}$ samples. This allows to further constrain the overall JES in a simultaneous fit to m_t and m_W.

CDF and D0 applied several sophisticated techniques in measurements of m_t. The major methods are "template" and "matrix element" approaches. CDF performed the template analysis using lepton+jets channel and 680 pb^{-1} [17]. The event sample has been selected using requirements similar to those described above for their cross section measurement (with jet p_{T} cuts depending on the b-tagging category of each event). A kinematic fit is used to decide the best value of m_t for each event after considering all parton-to-jet assignments and constraining the fitted W mass to the book value. The resulting m_t distribution is then compared to Monte Carlo m_t templates simulated for various top masses as illustrated in Fig. 9 (left). The final reconstructed top mass is determined from a simultaneous fit of the

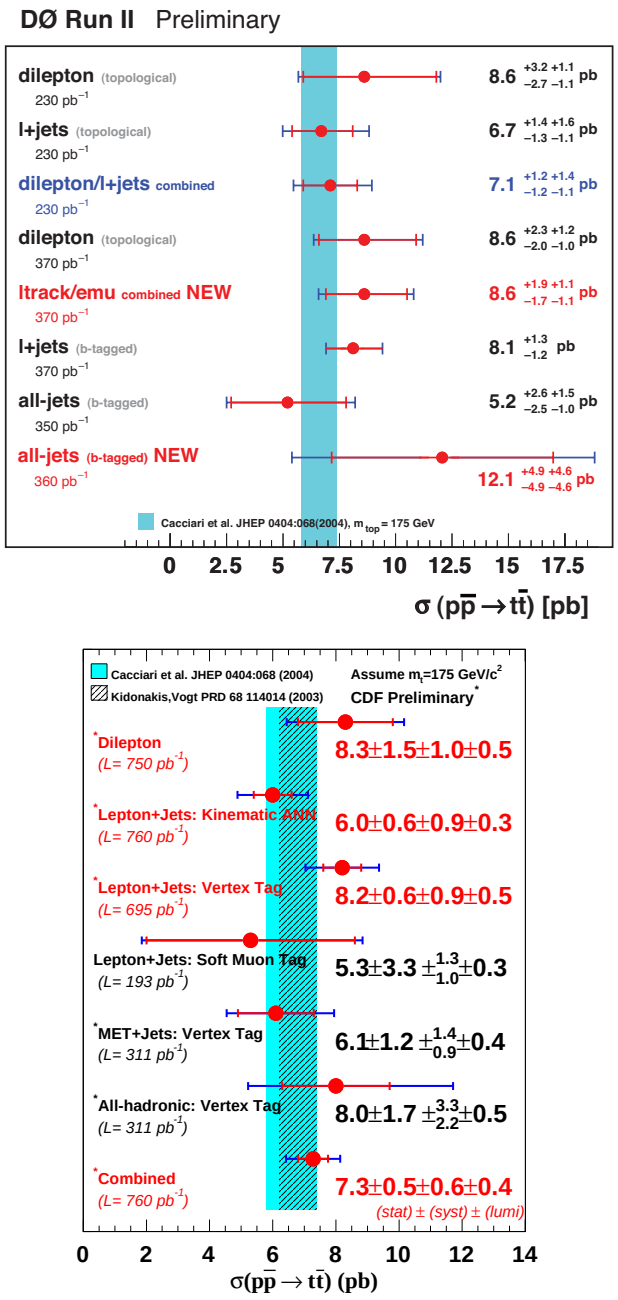


Fig. 8. Summary of recent $t\bar{t}$ cross section results from D0 and CDF.

templates to the observed distribution, as function of m_t and a shift in the jet energy scale, $\Delta_{\rm JES}$, Fig. 9 (right). The fit yields a top-quark mass of $m_t = 173.4 \pm 2.8$ GeV. The *in situ* calibration is consistent with the standard calibration but reduces the JES-related uncertainty by $\approx 40\%$.

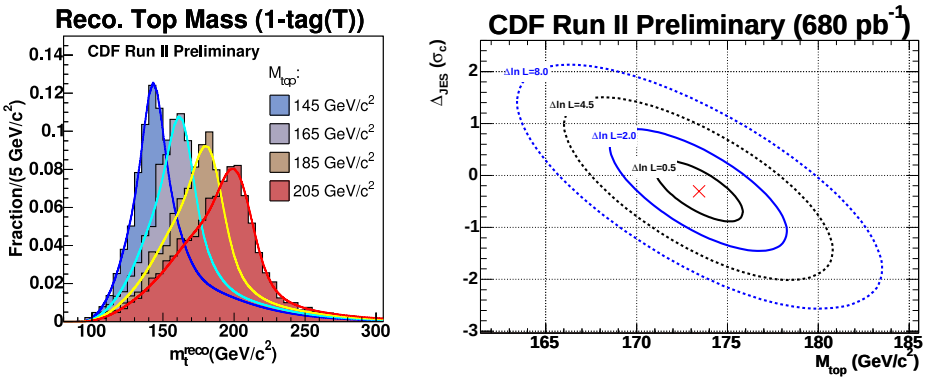


Fig. 9. Left: m_t templates from Monte Carlo. Right: Result of the template fit to lepton+jets data *versus* m_t and $\Delta_{\rm JES}$.

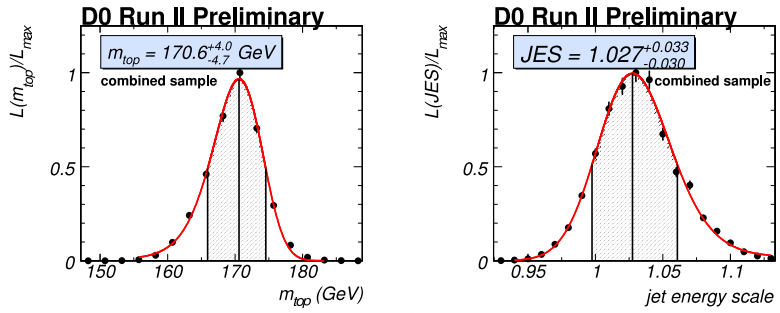


Fig. 10. Likelihood distributions *versus* m_t (left) and $\Delta_{\rm JES}$ (right), and the 68% confidence-level (C.L.) intervals, using the ME method and b-tagging information.

D0 developed the matrix element (ME) method in Run 1 and applied it to 370 pb^{-1} of Run 2 data [18]. In this method the probabilities for an event to be $t\bar{t}$ signal or the dominant W+jets background are calculated using the corresponding LO matrix elements. The probabilities of all events are combined into a final likelihood, which is then maximized as a function of m_t and an overall JES factor (in the Run 2 implementation). The likelihood distributions for both parameters are shown in Fig. 10. The result using the b-tagging information is $m_t = 170.6^{+4.0}_{-4.7}(\text{stat.} + \text{JES}) \pm 1.4(\text{syst.})$ GeV.

Fig. 11 (left) summarizes the best independent top-quark mass measurements from CDF and D0 [19]. The combination of published Run 1 measurements with the recent preliminary Run 2 results using up to 1 fb^{-1} of data yields a preliminary world average mass of the top quark $m_t = 171.4 \pm 2.1$ GeV. The top-quark mass is now known with a precision of 1.2%. The precise measurements of the top and W masses can be used to constrain the value of m_H, as illustrated in the right panel. They suggest a low value of the mass of the Higgs boson setting the stage for an exciting race between Tevatron and LHC experiments towards its discovery.

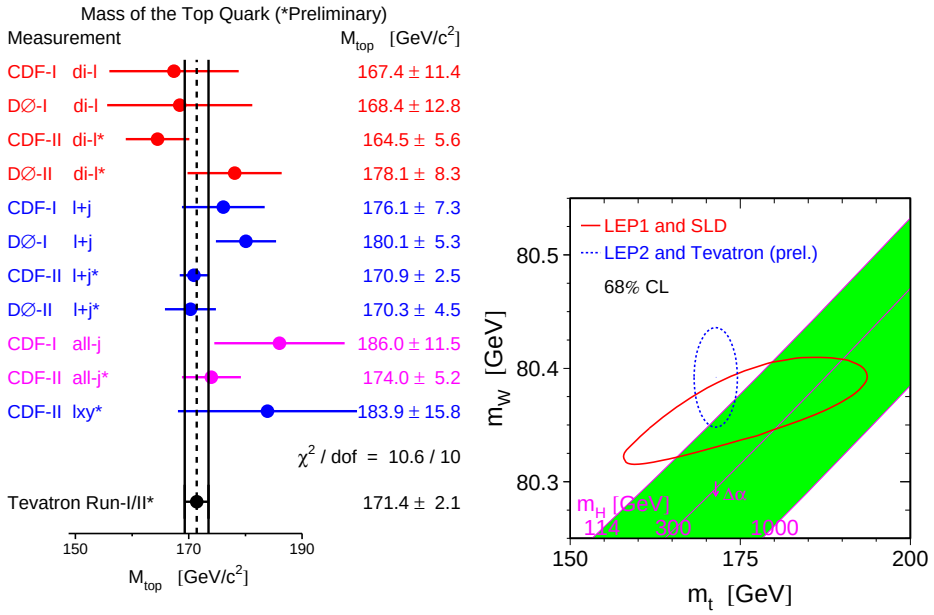


Fig. 11. Left: Combination of best independent measurements of m_t. Right: Constraints on m_H from global electroweak SM fits in the m_t and m_W plane.

D0 and CDF have searched for a narrow-width heavy resonance X decaying into top-quark pairs [20]. Such resonant $t\bar{t}$ production is expected *e.g.* in various "topcolor" models. The $t\bar{t}$ invariant mass spectrum from D0 is shown in Fig. 12 (top). This analysis is based on lepton+jets channel using a lifetime tag to identify b-quarks in 370 pb^{-1}of data. No evidence for a $t\bar{t}$ resonance X was found by either collaboration and upper limits on $\sigma_X \times B(X \to t\bar{t})$ have been derived as a function of m_X (Fig. 12 (bottom) for D0 results). For a topcolor Z' model [21], the existence of a leptophobic Z' boson with mass $m_{Z'} < 680$ (725) GeV has been excluded by D0 (CDF) at 95% C.L., for $\Gamma_{Z'} = 0.012 m_{Z'}$.

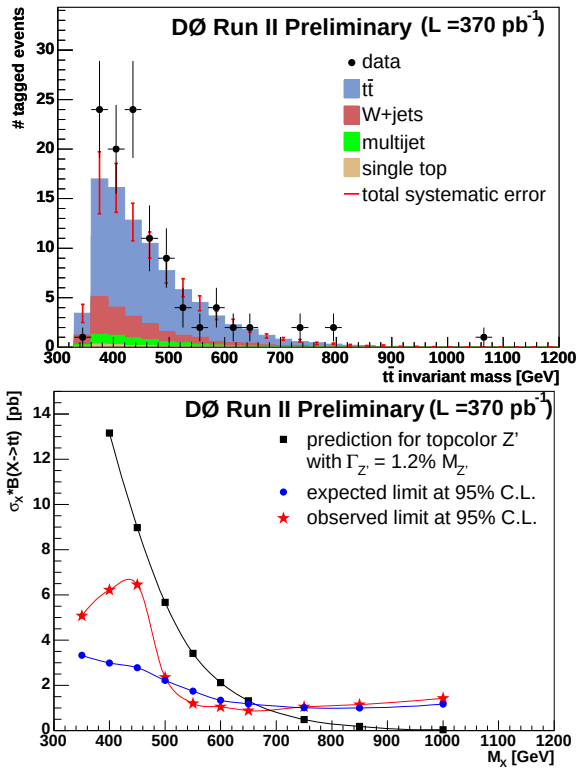


Fig. 12. Top: $t\bar{t}$ mass distribution in lepton+jets channel. Bottom: 95% C.L. upper limits on $\sigma_X \times B(X \to t\bar{t})$ compared to a prediction for a topcolor Z'.

Using 320 pb^{-1}, CDF searched [22] for the $W^+W^-b\bar{b}b\bar{b}$ signature of the associated $t\bar{t}H$ production. This process is expected to help the discovery of a light Higgs and provide a determination of the t–H coupling at the LHC. The CDF analysis required a p_{T}> 20 GeV/c e or μ candidate, five or more jets with $E_{\mathrm{T}} > 15$ GeV and $|\eta| < 2$, three or more b-tagged jets, and $\not\!\!E_{\mathrm{T}} > 10$ GeV. One candidate event was found (Fig. 13 (top)), consistent with the total expected background of 0.89 ± 0.12 events. The major contributions to background were from mistagging a light-quark jet as a b-jet, QCD multijet events where a jet fakes a lepton, and irreducible backgrounds from SM sources (including $t\bar{t}b\bar{b}$, $t\bar{t}c\bar{c}$ *etc.*). CDF obtained the first experimental limit on $\sigma_{ttH} \times B(H \to b\bar{b})$ of 660 fb, weakly depending on m_H (Fig. 13 (bottom)). The expected $t\bar{t}H$ signal is 0.024 ± 0.005 events for $m_H = 115$ GeV.

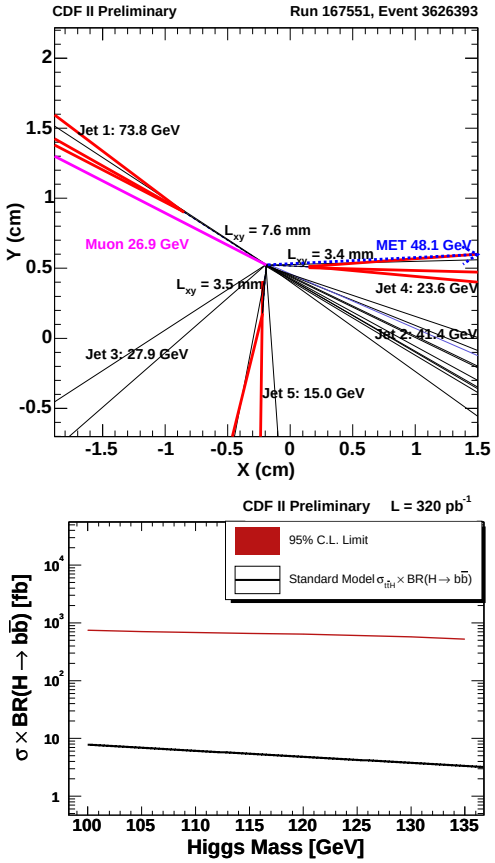


Fig. 13. Top: $t\bar{t}H$ candidate event from CDF. Bottom: 95% C.L. upper limit and SM prediction for $\sigma_{ttH} \times B(H \to b\bar{b})$ *versus* m_H.

3. Conclusions

Tevatron measurements advance the understanding of "soft" and "hard" aspects of QCD including higher-order processes and multi-jet radiation; facilitate development and tuning of perturbative and Monte Carlo tools; improve understanding of PDFs, jet algorithms and calibrations. Building upon this progress and using large data samples that have become available in Run 2, top-quark studies have entered a precision era, providing determination of $t\bar{t}$ cross section approaching 10% precision and of the top mass nearing 1%. Advanced analysis methods have been developed and tried in the hadron-collider environment. The experience from the Tevatron is an extremely valuable resource and it can greatly benefit the "rediscovery" of the Standard Model and searches for new physics at the LHC.

REFERENCES

[1] V.M. Abazov *et al.*, *Phys. Lett.* **B639**, 151 (2006).

[2] T. Binoth *et al.*, *Eur. Phys. J.* **C16**, 311 (2000); S. Catani *et al.*, *J. High Energy Phys.* **05**, 028 (2002).

[3] A. Abulencia *et al.*, *Phys. Rev. Lett.* **96**, 122001 (2006); CDF Note 8388 (2006).

[4] W. Giele *et al.*, *Nucl. Phys.* **B403**, 633 (1993).

[5] V.M. Abazov *et al.* (D0 Collaboration), *Phys. Rev. Lett.* **94**, 221801 (2005).

[6] M.L. Mangano *et al.*, *J. High Energy Phys.* **0307**, 001 (2003).

[7] T. Gleisberg *et al.*, *J. High Energy Phys.* **0402**, 056 (2004).

[8] Z. Nagy, *Phys. Rev. Lett.* **88**, 122003 (2002); *Phys. Rev.* **D68**, 094002 (2003).

[9] G. Corcella *et al.*, *J. High Energy Phys.* **0101**, 010 (2001).

[10] T. Sjöstrand *et al.*, *Comput. Phys. Commun.* **135**, 238 (2001).

[11] D. Acosta *et al.*, CMS Note 2006-067 (2006).

[12] D0 Note 5066-CONF (2006).

[13] CDF Note 8381 (2006).

[14] N. Kidonakis, R. Vogt, *Phys. Rev.* **D68**, 114014 (2003); M. Cacciari *et al.*, *J. High Energy Phys.* **404**, 68 (2004).

[15] CDF Note 8110 (2006).

[16] D0 Note 5057-CONF (2006).

[17] CDF Note 8125 (2006).

[18] D0 Note 5053-CONF (2006).

[19] Tevatron Electroweak Working Group, `hep-ex/0608032`.

[20] D0 Note 4880-CONF (2006); CDF Note 8087 (2006).

[21] R.M. Harris, C.T. Hill, S. Parke, `hep-ph/9911288`.

[22] `http://www-cdf.fnal.gov/∼slai/ttH_public.html`